

# Atomistic Modeling of Defect Nucleation and Reaction: Transition from Bulk to Nanostructures

Jinpeng Chang\*, Ting Zhu\*, Ju Li<sup>+</sup>, Xi Lin\*, Xiao-Feng Qian\*, Sidney Yip\*<sup>#</sup>

\*Department of Nuclear Engineering, Massachusetts Institute of Technology, Cambridge, MA 02139-4307 (USA)

<sup>+</sup>Department of Materials Science and Engineering, Ohio State University, Columbus OH 43210-1178 (USA)

<sup>#</sup>Department of Materials Science and Engineering, Massachusetts Institute of Technology, Cambridge, MA 02139-4307 (USA)

This paper is published in IUTAM Symposium on Mesoscopic Dynamics of Fracture Process and Materials Strength, eds. H. Kitagawa and Y. Shibutani, Solid mechanics and its applications 115 (Kluwer, Dordrecht, 2004). ISBN: 1-4020-2037-6.

## INTRODUCTION.

We cite recent theoretical, molecular dynamics and finite-element studies of dislocation nucleation in nanoindentation [1-3] and electronic-structure calculations of ideal shear strength [4] to suggest that atomistic simulations in which interatomic bonds are broken and formed can provide mechanistic insights common to the mechanical failure and chemical reactivity of nanostructures. The critical information is the distribution of charge densities at saddle-point configurations, particular arrangements of ions and electrons where the system is on the verge of structural instability or chemical reaction. Here two additional problems are considered to expand on our simple notion. Homogeneous nucleation of deformation twinning [5] shows that the response of a perfect lattice to shear is sensitive to the energetics of bond strain. The interaction between a water molecule and a silica nanorod is an example where charge transfer has to be treated explicitly, no matter how approximately. Taken together they serve to motivate a holistic description of mechanical and chemical behavior which is appropriate for bulk solids, as well as nanostructures.

The aim of this contribution is to examine the common issues between the mechanics of large-strain deformation and the chemical dynamics of dissociative/associative reactions in the context of modeling materials structures of different length scales. The connection we seek stems from the simple observation that materials failure and reaction kinetics are quite different physical phenomena, yet when analyzed at the atomic level they are both governed by the action of the valence charge densities in the system. Multiscale modeling studies in the area of mechanics of materials have largely focused on linking atomistic simulations with mesoscale or continuum methods. Usually electronic degrees of freedom are not treated explicitly, except in first-principles calculations on perfect crystals where lattice symmetry can be exploited, or small-scale defects involving only tens of atoms. Problems of kinetics and dynamics of chemical reactions, by and large, have not attracted much attention in the modeling and simulation community. Also, there seems to be little discussion of a common perspective for understanding traditionally soft materials on the same footing as metals, semiconductors, and ceramics. In view of this situation we feel that there are particular challenges at the interface of mechanics and chemistry that can be posed through a focus on transition from bulk to nanostructures in atomistic simulation, realizing at the same time that this would also imply a transition from hard to soft matter. This is admittedly a fuzzy notion which needs to be firmed up with specific studies.

The challenges of combining mechanics and chemistry, bulk and nanostructures, hard and soft materials, all within a unifying framework are of course already part of the broad vision

of multiscale modeling, which has been articulated in various versions [6-8]. In the first study discussed here, it will be seen that the atomistic details of homogeneous nucleation of twinning obtained by atomistic simulations are revealing; however, being based on empirical classical interatomic potentials they need to be validated by electronic-structure calculations. In the second study, that of water-silica reaction in a highly strained environment, the feasibility of quantifying the effects of bond strain on the kinetics of hydration is demonstrated. To give an example of modeling functional properties of nanostructures that requires the calculation of charge density distribution, we consider briefly electron transport across a molecular junction. We also note that if a nanoscale device were to be of practical use, being able to predict its electrical conductivity would not be sufficient, the mechanical integrity of the junction would eventually have to be investigated.

## DEFORMATION TWINNING

Twinning and slip are the two primary plastic deformation mechanisms by which crystals can accommodate large strains. Deformation twins have long been identified in bcc, hcp and lower symmetry metals and alloys; more recently they have been found in fcc metals and alloys, in ordered alloys and other inter-metallic compounds, in elemental semiconductors and compounds, in non-metallic compounds such as calcite, and even in complex minerals and crystalline polymers [9]. The deformation is often characterized by very rapid formation of twinned regions, and large load drops in the stress-strain response; it operates generally at low temperatures, high stress, high strain rate, and in crystals of lower symmetry where the number of slip systems is limited. Schematically one can contrast slip and twin as lattice responses to shear where the relative displacement between two adjacent layer occurs only once in the case of slip. In the case of twinning the relative displacements between adjacent layers occur in a stack of at least two layers, see Figure 1.

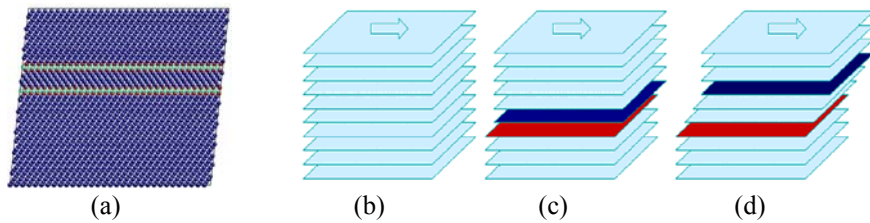


Figure 1 Atomic configuration of a twinned region in a crystal lattice enclosed by the twin boundaries, atoms are color coded according to local strain (a). Schematics depicting an undeformed stack of crystal planes prior to shear in the direction indicated by the arrow (b), deformation by slip (c), and deformation by twinning of four layers (d).

Similar to most first-order lattice phase transformations, twinning is typically separated into nucleation and growth stages. A twin nucleus may be formed by the action of an applied stress in a region of near-perfect crystal (homogeneous nucleation), or formed from a pre-existing defect configuration (heterogeneous nucleation). While the latter is more commonly observed, the former can occur in highly perfect specimens, e.g., in cadmium and zinc [10], where the stresses required are an order of magnitude higher. In the present study we are concerned with the molecular dynamics simulation of homogeneous nucleation of twinning in bcc Mo using the EAM-potential of Finnis and Sinclair [11].

Our simulation cell with periodic boundary conditions is chosen with the X (horizontal), Y (normal to plane of paper) and Z (vertical) axes along  $[111]$ ,  $[\bar{1}2\bar{1}]$ , and  $[10\bar{1}]$  respectively. The corresponding dimensions are 199Å, 198.6Å, and 192.7Å (500,000 atoms). Shear is applied at a constant rate of  $3 \times 10^6 \text{ s}^{-1}$  on the xy plane in the  $[111]$  direction (twinning direction). At 10 K

we observe homogeneous twin nucleation at a shear stress of 12.2 GPa (7.84% strain). Once nucleation sets in, a sharp decrease in strain energy and shear stress is observed. From a sequence of the instantaneous atomic configurations, shown in Figure 2, the twinned region (nucleus), delineated by color coding according to local strain and coordination, is seen to evolve into an oblate ellipsoidal shape (disk like). The disk is thickest in the middle while its edges are as thin as one layer. The defect can be described as a twinning dislocation loop with a burgers vector of  $\bar{b}/3$ , with  $\bar{b} = (a/2)[111]$ . From the MD results we estimate the velocity of the loop while the disk is expanding to be  $\sim 6000$  m/s (sound speed is 6000-7000 m/s). Expansion in the  $\{112\}$  plane is much faster than the out-of-plane growth, the fact that the former is also anisotropic causes the shape projected on the plane to be elliptical. Across the twinned region, one can verify the relative displacements are distributed in the form of  $(0, \dots, 0, b/3, \dots, b/3, 0, \dots, 0)$ , which is in accordance with Figure 1.

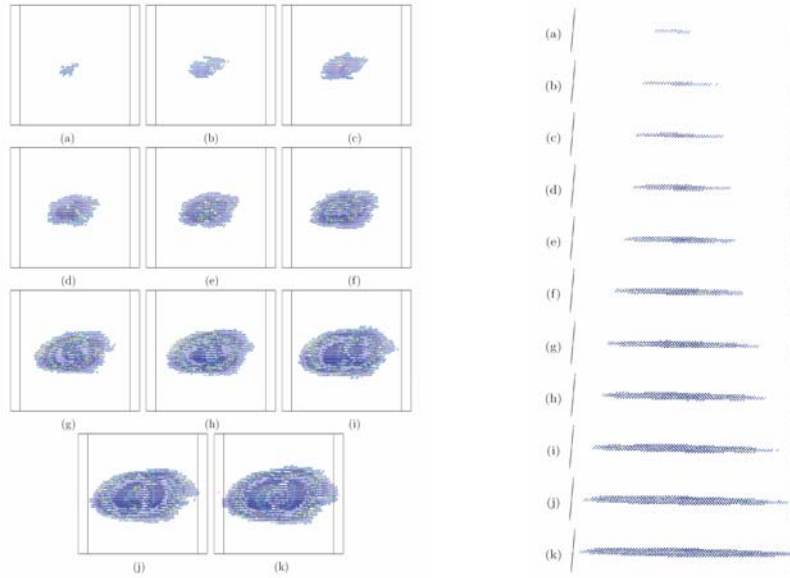


Figure 2. Growth of a disk-shape nucleus of a twinned region observed in MD simulation of shear deformation, top view (left) and side view (right).

To interpret the simulation results we introduce a 1-D chain model to represent the essential structural characteristic of the twin defect. As shown in Figure 3, the defect is a chain of 'model atoms' specified by a set of coordinate  $x_i$ , measured on the X-axis in direction  $[111]$ . Associated with a 'model atom'  $i$  is a layer of physical atoms, the plane being perpendicular to the chain direction, with coordinates  $(x_i, y_i, z_i)$ . In the chain model the only relevant degrees of freedom are the *relative displacements* in the  $[111]$  direction *between adjacent layers*, that is,  $\Delta x_i = x_{i+1} - x_i$ . If the twin structure is composed of  $N$  nonzero relative displacements of 'model atoms' ( $N$  planes of atoms are displaced *successively*), we would have  $N$  *primary* degrees of freedom,  $\Delta x_i$ ,  $i = 1, \dots, N$ , specifying the defect. The other degrees of freedom, relative displacements in the Y and Z directions,  $\Delta y_i$  and  $\Delta z_i$ , will be considered as *secondary*. In principle, the latter should be allowed to relax during deformation; however, one may anticipate that in a first approximation such relaxations can be neglected for the sake of computational simplicity. Whether these relaxations are actually ignored or not, our purpose is to investigate the structure-energy relation of the 1-D chain model by considering the variation of the system

energy only with the primary degrees of freedom. In other words, for the system energy we would write  $E = E(0, \dots, 0, \Delta x_j, \dots, \Delta x_{j+N}, 0, \dots, 0)$ , with the N successively displaced planes starting at position j and ending at j+N.

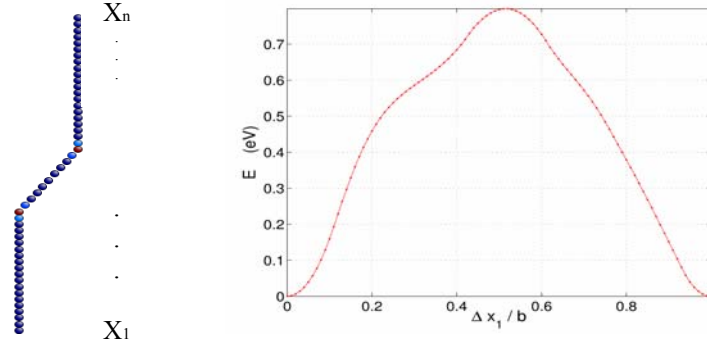


Figure 3. Schematic of the 1-D chain model of twinning (9 layers in this example). Variation of strain energy with relative displacement of the  $(\bar{1}\bar{1}2)[111]$  twin in a 1-layer shear (the  $\gamma$ -surface) with Y and Z relaxations.

The simplest case one can consider is the 1-layer shear, the rigid translation of the upper half of the lattice relative to the lower half. The energy  $E(0, \dots, \Delta x_1, \dots, 0)$  with relaxation in the other two directions taken into account is shown in Figure 3. This is just the conventional  $\gamma$ -surface energy in the  $[111]$  direction. The energy barrier is 0.82eV. Critical stress in the positive direction is 33 GPa while in the negative direction it is 29 GPa, indicating an expected asymmetry at approximately  $\Delta x_1 = b/2$ . One can discern a softening around  $\Delta x_1 = b/3$ , but this did not lead to a metastable state. However, the value of the relative displacement is close to the critical value for twin nucleation, as we will see in the case of 2-layer shear below. Two other remarks are in order. First, we have checked that without relaxation the energy curve peaks at a slightly higher value, 0.84eV, and a lower displacement, which are not surprising. Secondly, repeating the calculation for  $[111]$  shear on the  $(\bar{1}10)$  gives a symmetric curve with a much lower barrier, 0.42eV, at  $b/2$ , and corresponding stress of 15.13GPa. These results are again reasonable in view of the fact that  $(\bar{1}10)[111]$  is a primary slip system.

For the 2-layer shear we show the energy surface in Figure 4 where a minimum is now seen around the displacements  $(b/3, b/3)$ . Under positive shear the system can either twin or slip. The energy barrier for twinning is 0.672eV with saddle point at  $(0.36b, 0.16b)$ , while for slip the barrier is 0.736eV with saddle point at  $(0.5b, 0.09b)$ . Under negative shear, only slip is allowed, at a barrier of 0.808eV. It is also useful to display the energy surface in the form of contour plot, see Figure 4. Knowing the energy contour one can trace out the minimum-energy path for the two deformations, twin and slip. In Figure 4 we see connections between starting configuration at the perfect lattice energy minimum  $(0,0)$  and the two ending configurations, an energy minimum corresponding to the 2-layer twin at  $(b/3, b/3)$ , and another minimum corresponding to slip at  $(b, 0)$ . The two paths bifurcate at  $(0.29b, 0.03b)$  before either of the saddle points is encountered. The system can either twin or slip after the bifurcation point; however, since the twinning path has a lower energy barrier, 0.672eV, than the slip path, with barrier of 0.736eV, twinning will be favored. For comparison we have also performed energy surface calculations for the  $(\bar{1}10)[111]$  slip system. The only energy minima found are at  $(0,0)$ ,  $(b,0)$ ,  $(0,b)$ , and  $(b,b)$ , which means there is no twin minimum and the only system response to shear is slip. In this case

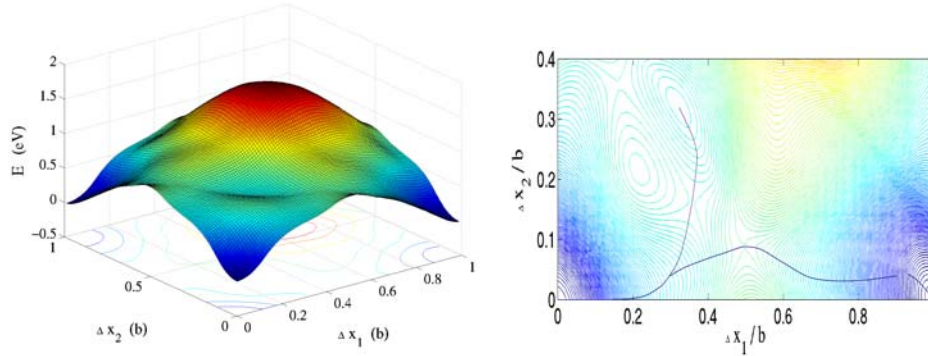


Figure 4. Strain energy surface (left) and energy contour plot (right) for the  $(\bar{1}\bar{1}2)[111]$  deformation, with  $Y$  and  $Z$  relaxations, in a 2-layer analysis [5]. An energy minimum at relative displacements of  $b/3$  for sliding between adjacent layers confirms the existence of twin defect in the present model for bcc Mo.

the energy surface is completely symmetric about  $(b/2, b/2)$ . Comparing the energy barriers for the two  $(\bar{1}10)[111]$  and  $(\bar{1}\bar{1}2)[111]$  slip systems, we have 0.422eV vs. 0.736eV. This is consistent with the fact that the former is the primary slip.

The structural and energy details we have discussed have qualitative and quantitative significance only to the extent that the interatomic potentials used in the simulation are adequate in representing the interaction energies associated with the chemical bonds. While empirical potentials like the Finnis-Sinclair model are known to give a reasonable description of the crystal lattice, in its equilibrium configuration or elastically deformed, their accuracy in describing large-strain processes such as dislocation or twin nucleation is less assured. Thus, the foregoing results should be regarded as only qualitatively meaningful; quantitative details such as activation barriers and critical stresses will have to be deferred to electronic-structure calculations at the level of density functional theory [4]. On the other hand, even without having the twin nucleation results at the first-principles in hand we can already say that deformation studies involving charge density distributions will be very informative from the standpoint of basic understanding of material deformation and failure.

## WATER-SILICA REACTION IN A STRAINED NANOROD

The ability to probe the dynamics of bond breaking and formation and the influence of local chemical environments presents an opportunity to model properties of nanostructures under conditions of their synthesis and performance. We are currently investigating the chemical reactivity of a nano-rod of  $\text{SiO}_2$  when it comes into contact with water [12]. By following the reactions as kinetic events involving the redistribution of charge densities, we expect to gain insight into the question of how bond strain, induced by stress or thermal environment, can affect reactivity.

It is our belief that a nanorod of atoms, as a novel standalone structure, presents significant advantages relative to a cluster or bulk lattice. Unlike a cluster its mechanical behavior can be meaningfully extracted and scaled up continuously to larger dimensions. The rod is also more suitable than an extended lattice for the characterization of effects of stress and chemical reaction because of better control over the nucleation site for structural defect and chemical bond reaction. For example, introducing a notch in the nanorod gives a well defined site for stress concentration or strain localization, as well as for chemical reaction. As for computational burden, the rod and cluster are comparable in that both are much less

computationally intensive than bulk. The hundred or so atoms involved are just about manageable for first-principles methods.

We have constructed a silica nanorod composed of 144 atoms (48  $\text{SiO}_2$  molecules) by stacking a number of  $\text{Si}_6\text{O}_{18}$  rings and capping the two ends to eliminate any dangling bonds [12]. Using a potential description consisting of pair and Coulomb interactions [13], we have performed uniaxial tension and compression simulations on the nanorod and have observed the effects of temperature on the failure mechanism. The stress-strain responses of the nanorod, with and without a notch, as it is strained to rupture are shown in Figure 5. Also shown are the atomic configurations of the initial structure of the notched nanorod and the same rod in a highly deformed state just prior to rupture. It is noteworthy that the rod thins down to a single chain of atoms before breaking. This appears to be a characteristic mode of failure that has been recently observed in gold nanojunctions by *in situ*, real time resolved high-resolution TEM [14]. It is also interesting to contrast this behavior with the response of larger notched structures would behave under the same tensile loading [15], shown in Fig. 6..

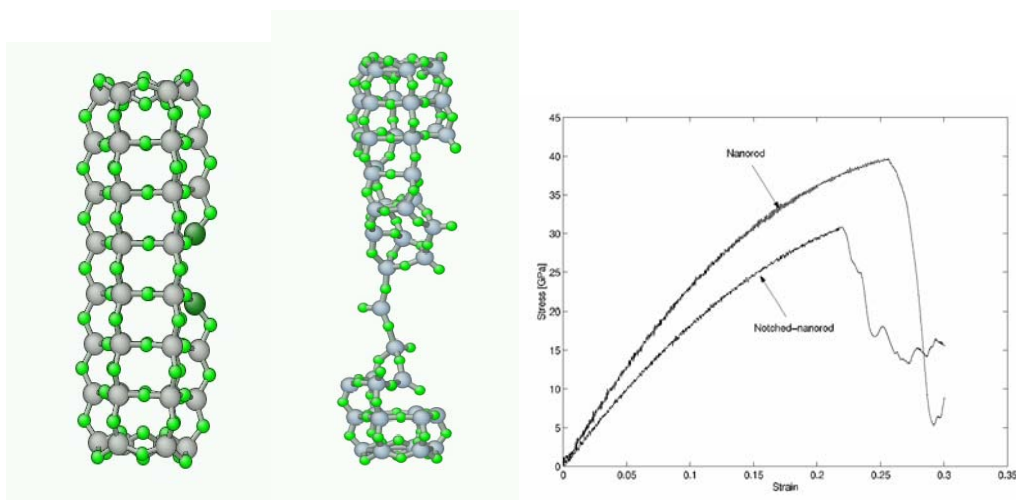


Figure 5. Tensile rupture of a quartz nanorod at 100K, atomic configurations of initial notched structure and deformed rod prior to rupture, and stress-strain responses with and without the notch.

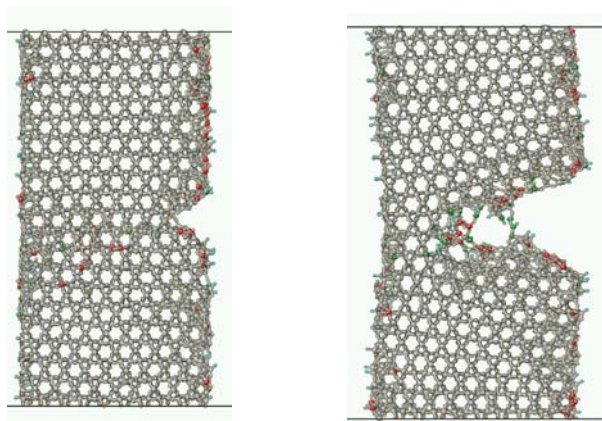


Figure 6. Atomic configurations of a quartz crystal with a surface notch under tensile deformation (vertical direction)[15].

To investigate the sensitivity to chemical reaction of a strained nanorod we consider the effect of water in contact at the surface of the rod. Our interest is probe the kinetic pathways of a

water molecule reacting with a strained Si-O bond. That the presence of water has a significant effect on strength of quartz, particularly at high temperature, is widely known as the problem of 'hydrolytic weakening'. It was first proposed that the fundamental mechanism for this effect is the hydrolysis of a siloxane bond, which bridges two neighboring SiO<sub>4</sub> tetrahedra, to form two terminal SiOH silanol groups [16]. The silanol groups are believed to facilitate bond rupture and thus lower the strength of silica. Since the process involves bond breaking and formation, and significant effects of charge transfer, classical potential simulations will not be adequate. For initial exploration we focus on the reaction between a water molecule and a silica nanorod which is held in various stages of uniaxial tension. Interaction energies and forces are obtained by a semi-empirical molecular orbital method as coded in a general-purpose package MOPAC [17].

To identify the transition state and reaction pathways we adopt the Nudged Elastic Band method [18] of locating the saddle point configuration and the associated energy barrier. We show in Figures 7 and 8 the reaction pathway at the stress level of 16.7 GPa and the corresponding minimum energy path. These results suggest a three-step mechanism for the hydrolysis process. (1) As can be seen in Figure 7(b), a metastable adsorbed state is first formed. It corresponds to a local energy minimum point b in Figure 8. (2) A proton is transferred to the bridging O<sub>br</sub> atom. A new bond between O<sub>br</sub> and H is formed, while the original bridging bond between H and O<sub>w</sub> is eliminated. The saddle point configuration corresponding to this proton transfer process is shown in Figure 7(c). This configuration has the maximum energy barrier on the minimum energy path, as represented by point c in Figure 8. (3) Rupture of the bond between bridging O<sub>br</sub> and Si occurs to yield surface Si-O-H groups as shown in Figure 7(d). The system reaches a local energy minimum represented by the point d in Figure 8.

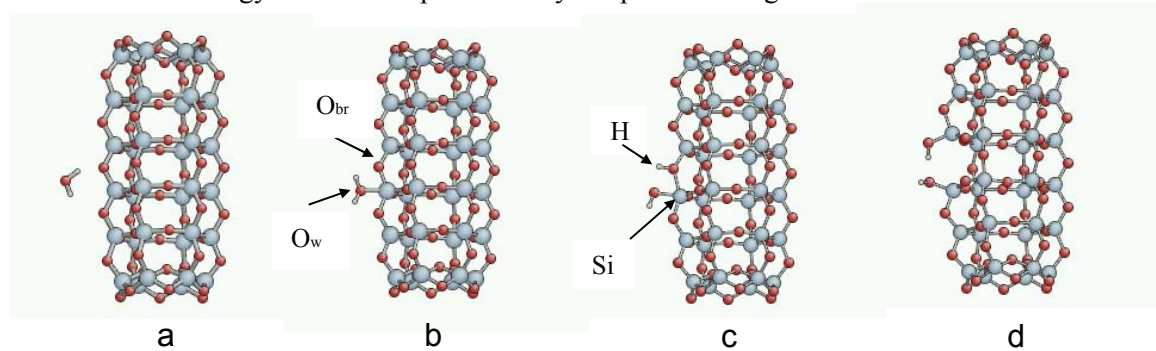


Fig. 7. Reaction pathway for a nanorod, strained at 16.7 GPa, being attacked by a water molecule.

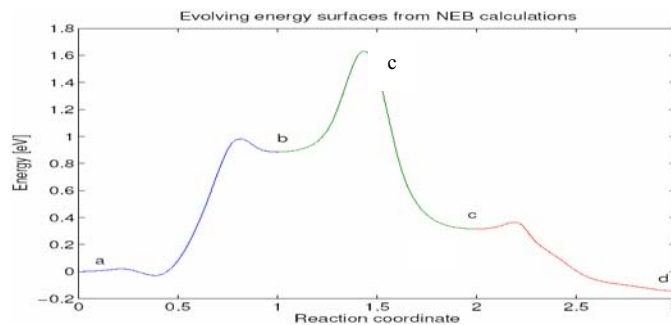


Fig.8. Minimum energy path from Nudged Elastic Band calculation.

From the minimum energy path calculation, an activation energy barrier  $\Delta E$  at the present stress level (16.7 GPa) is obtained,  $\Delta E = 1.6$  eV. As a rule of thumb, at room temperature a transition process with an energy barrier around 0.5 eV will occur about every 1ms. Therefore, hydrolysis at the present stress level is unlikely to occur on a laboratory timescale at room temperature and the present stress level. However, if the temperature were to increase three-fold,

from 300K to 900K which is then close to the temperature in the original experiment on hydrolytic weakening, the possibility for hydrolysis of Si-O bond will significantly increase.

## MODELING FUNCTIONAL NANOSTRUCTURES

As a result of current interest in nanoscience and technology, significant opportunities are being created for understanding the physical, chemical (and biological) properties of materials structures intermediate between isolated atoms and molecules and bulk matter. Novel structures displaying unusual phenomena and functional properties have been observed on the nanoscale (a fraction of nm to 100 nm) along with developments of new experimental, theoretical and simulation tools. An example is the electrical conductance across a molecular junction. Although the notion of a single organic molecule acting as an electronic rectifier had been discussed in 1974 [19], it was only in the early '90s that the prospect of building electronic circuits at the level of single molecules was recognized [20]. More recently interests in the conductivity behavior of a molecular junction have intensified considerably when it was realized that thiol-terminated conjugated oligomers in the form of a self-assembled monolayer could exhibit such transport behavior [21]. A specific issue which cannot be resolved by experiments is the mechanism of electron migration across a metal-molecule-metal interface, such as a junction consisting of a thiol terminated benzene ring in contact with a Au atom at each end, as shown in Figure 9. The theoretical determination of the current- voltage characteristics of this system is

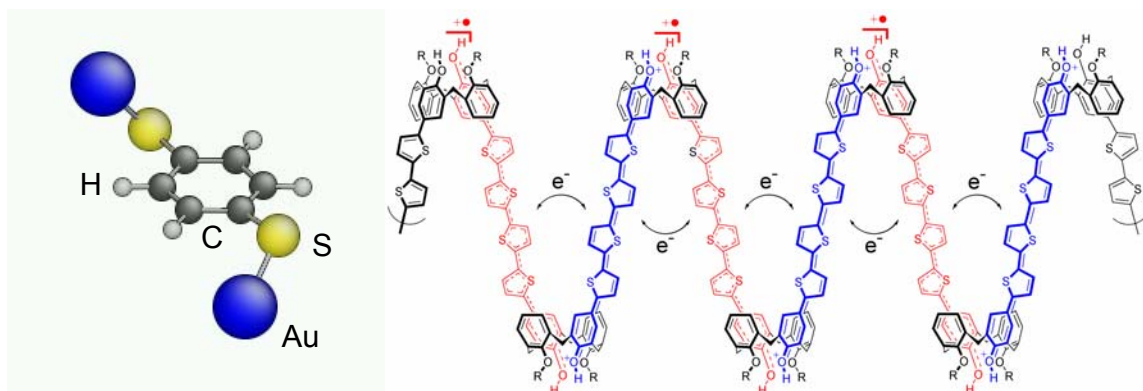


Figure 9. A molecular junction model in the form of a Au-S-(p-C<sub>6</sub>H<sub>4</sub>)-S-Au system is shown on the left, while on the right hinge molecules (calix[4]arene) are connected to rigid rods of quarterthiophene to form a structure that can function as a molecular actuator.

made all the more difficult by the contact effects between metallic tips and single molecules. As a result, band-structure methods developed for bulk phases cannot be applied directly while quantum chemistry techniques for molecules are by themselves also inadequate. One approach being investigated is the Green's function scattering formalism combined with density functional theory (Kohn-Sham) Hamiltonian which treats electron correlation and nonlocal exchange [22]. The Kubo-Greenwood formula in linear response theory, which emphasizes electronic scattering and interference, is used for condensed phases [23]. In our opinion this is not likely to succeed because it gives essentially a volume average, whereas the relevant characteristics of the junction is highly local. An approach we are currently investigating is to propagate a wave packet across the junction by numerically solving the time-dependent *Schrödinger* equation.

The molecular junction we have just mentioned is one example of a class of nanostructured conjugated polymers that are being synthesized and characterized for device applications (the organic analogue of Si) [24]. A somewhat more complicated structure is the thiophene-based conducting polymer, shown also in Figure 9, which is being considered as a



candidate for molecular actuator. In this case hinge molecules (cones of 4 six-member rings in various conformations) tie together rigid rods (chains of four 5-member rings, including a sulfur atom) to form a polymer backbone that can contract or expand depending on the oxidation state (the rods attract each another in the oxidized state) [25]. Since the conductivity of this system is obviously also a property of interest, the need for an appropriate method to analyze electron transport in organic nanostructures is therefore quite general. One can go even further by noting that conductivity is one of several materials properties that are fundamental to the understanding and development of nanodevices, the others would include modulus, mobility, strain, and response time.

**Acknowledgements.** This work was supported by the Air Force Office of Scientific Research, the Defense Advanced Research Program Agency-Office of Naval Research, Honda R&D, Inc., and the National Science Foundation (KDI and ITR). We acknowledge the collaboration of Jean-Paul Crocombette in the conductivity study.

## References

1. J. Li, K. J. Van Vliet, T. Zhu, S. Yip, S. Suresh, *Nature (London)* **418**, 307 (2002).
2. K. J. Van Vliet, J. Li, T. Zhu, S. Yip, S. Suresh, *Phys. Rev. B* **67**, 104105 (2003).
3. T. Zhu, J. Li, K. J. Van Vliet, S. Suresh, S. Yip, *J. Mech. Phys. Solids*, submitted.
4. S. Ogata, J. Li, S. Yip, *Science* **298**, 807 (2002).
5. J. Chang, PhD Thesis, MIT, June 2003.
6. G. H. Campbell et al., *Mater. Sci. Eng. A* **251**, 1 (1998).
7. *J. Comp. Aid. Mater. Des. (Special Issue)* **6** (1999).
8. S. Yip, *Nature Mater.* **2**, 3 (2003).
9. J. W. Christian and S. Mahajan, in *Progress in Materials Science* (Elsevier, 1995), vol. 39, p. 1.
10. P. B. Price, *Proc. Roy. Soc. A* **260**, 251 (1961).
11. M. W. Finnis and J. E. Sinclair, *Phil. Mag. A* **50**, 45 (1984).
12. T. Zhu, J. Li, S. Yip, R. J. Bartlett, S. B. Trickey, N. H. de Leeuw, *Mol. Sim.*, in press.
13. B. W. H. van Beest, G. J. Kramer, R. A. van Santen, *Phys. Rev. Lett.* **64**, 955 (1990).
14. V. Rodrigues and D. Ugarte, *Phys. Rev. B* **63**, 073405 (2001).
15. D. Liao, PhD Thesis, MIT, August 2001.
16. D. T. Griggs and J. D. Blacic, *Science* **147**, 292 (1965).
17. MOPAC
18. G. Henkelman, B. P. Uberuaga, H. Jonsson, *J. Chem. Phys.* **113**, 9901 (2000).
19. A. Aviram and M. A. Ratner, *Chem. Phys. Lett.* **29**, 277 (1974).
20. 1991 mole-tronics papers.
21. M. A. Reed, C. Zhou, C. J. Muller, T. P. Burgin, J. M. Tour, *Science* **278**, 252 (1997), J. Chen, M. A. Reed, M. Rawlett, J. M. Tour, *Science* **286**, 1550 (1999), J. M. Tour, *Molecular Electronics* (World Scientific, Singapore, 2003).
22. P. A. Derosa and J. M. Seminario, *J. Phys. Chem. B* **105**, 471 (2001).
23. C. V. Landauro and H. Solbrig, *Physica B* **301**, 267 (2001), V. Recoules, P. Renaudin, J. Clereouin, P. Noiret, G. Zerah, *Phys. Rev. E* **66**, 056412 (2002).
24. E. Smela, presentation at ARO Workshop on Interface Mechanics, Raleigh, May 2003.